

# Phase-shift laser range finder based on high speed and high precision phase-measuring techniques

Pengcheng Hu<sup>1,#</sup>, Jiubin Tan<sup>1</sup>, Hongxing Yang<sup>1</sup>, Xiping Zhao<sup>1</sup> and Siyuan Liu<sup>2</sup>

1 Ultra-precision Optoelectronic Instrumentation Engineering Center, Harbin Institute of Technology, No.2 Yikuang Str., Harbin, Heilongjiang, China, 150080  
2 China Dfh Satellite Co., Ltd. 12/f, Shenzhou Mansion, No. 31, Zhongguancun South Str., Haidian, Beijing, China, 100094  
# Corresponding Author / E-mail: hupc.cn@gmail.com, TEL: +86-451-86412041-803, FAX: ++86-451-86412896

KEYWORDS : Dynamic measurement error, Dual channel digital phase measurement, Measurement speed, Phase-shift laser range finder

*High speed and high precision phase measuring techniques is proposed in this paper to further improve the dynamic measurement accuracy of phase-shift laser range finder. In the method, heterodyne processing is employed to convert the phase measurement of high frequency signal into that of intermediate frequency signal, and the dual channel digital phase measuring method is employed to improve the accuracy and rate of phase measurement, and finally the Kalman filter based state estimation is introduced to further suppress the static and dynamic error of the phase measuring. Experimental results show that, for a moving target at a velocity up to 200 mm/s, an uncertainty better than  $\pm 1.2$  mm can be achieved at a data rate up to 2 kHz ( $t=0.5$  ms) with a laser range finder using the proposed method.*

Manuscript received: January XX, 2011 / Accepted: January XX, 2011

## 1. Introduction

Laser range finders are widely used in the fields like spaceflight, robot vision, mapping, and mechanical manufacturing for their merits of being non-contact, high precision and low cost [1,3]. The three major techniques used for laser range finder are time of flight (TOF), frequency modulation continuous wave (FMCW) and phase-shift measurement. In these methods, phase-shift measurement can achieve higher resolution in a long distance [4-8].

However, for most of the phase-shift laser range finders available now, the accuracy of phase-measuring is always improved at the expense of low measurement rate and large measurement time. In addition, static algorithms such as the slide window average and the least squares estimate are also employed to further decrease measurement noise from photoelectric detection and phase detection. However, these strongly restrict the measurement rate and the real time property of the system, which makes it impossible to measure a moving target precisely.

In order to overcome problems mentioned above, a phase-shift laser ranging method based on high speed and high precision phase-measuring is presented. Firstly a dual channel digital phase meter is developed to improve the phase measuring rate. Secondly the Kalman filter based state estimation method is introduced to further suppress the static and dynamic error of the phase measuring.

## 2. Principle of phase-shift laser range finder

As shown in figure 1, a laser beam with intensity modulated at a particular frequency is emitted to the target, and reflected back. And phase-shift is produced in the received beam due to the time delay between the emitted point and the target [9].

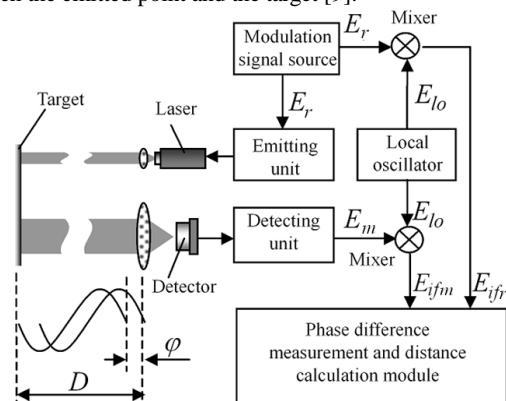


Figure 1. Block diagram of phase-shift laser range finder

Distance  $D$  can be obtained by measuring the phase-shift, and expressed as

$$D = \frac{c}{2f} \cdot \frac{\varphi}{2\pi} \quad (1)$$

Where  $c$  is the light velocity,  $f$  is the modulation frequency, and  $\varphi$  is the phase-shift between measurement signal and reference signal. When modulation frequency  $f$  is determined, the non-ambiguity range

for a laser range finder is  $D_{nar}=c/2f$ , and the resolution of distance measurement can be expressed as

$$\delta D_{\min} = \frac{c}{2f} \cdot \frac{\delta\phi_{\min}}{2\pi} \quad (2)$$

Equation (2) indicates that distance measurement resolution  $\delta D_{\min}$  is directly determined by the phase-shift resolution  $\delta\phi_{\min}$ . For example, measurement range  $D$  is 15m and the measurement resolution  $\delta D_{\min}$  is 2mm, when  $f=10\text{MHz}$  and  $\delta\phi_{\min}=0.05^\circ$ .

### 3. High speed and high precision phase measurement

Equation (1) shows that the phase-shift  $\phi$  between the measurement signal and reference signal must be measured accurately to obtain a precise distance measurement. Many phase measurement methods for phase-shift laser range finder have been proposed, such as lock-in amplifier based measurement, under-sampling techniques based measurement and auto-digital phase measurement [4-8]. The lock-in amplifier and under-sampling phase measurement can only get the phase difference from two signals with the same frequency. Because of the low measurement speed, they are not suitable for targets with fast movement. To improve the phase measurement accuracy, the auto-digital phase measurement usually processes the signals with heterodyne method which can convert two high frequency signals to low frequency signals. However, affected by drift of frequency, there are intolerable static measurement errors in the current heterodyne digital phase measurement [9]. At the same time, multicycle method is usually applied to reduce the  $\pm 1$  counting error in digital phase measurement. This increases the measuring time. It is reported that the dynamic error can achieve tens of millimeters when measuring the moving targets.

In order to improve the static and dynamic accuracy of phase-shift laser range finder, a high speed and high accuracy digital phase-measuring technique is presented. In this technique, the signals with high frequency are converted to intermediate frequency signals using heterodyne processing. Then the dual channel digital phase measuring method is employed to improve the accuracy and rate of phase measurement. And based on the constant-velocity model, a Kalman filter is designed to further improve the measurement accuracy.

#### 3.1 Heterodyne processing and digital conversion

As shown in figure 2, heterodyne processing can convert phase difference measurement of high frequency signals to that of low frequency signals. i.e. let the reference and measurement signal frequency mixing with local oscillator signal at the same time. Supposing  $E_r=A_r\cos(2\pi f_r t+\phi_0)$  and  $E_m=A_m\cos(2\pi f_m t+\phi_0+\phi_x)$  are the signals at emission and reception unit.  $E_{lo}=A_{lo}\cos(2\pi f_{lo} t+\theta)$  is the local oscillator signal, the following signals are obtained by mixing these signals:

$$U_r = \frac{A_r A_{lo}}{2} \{ \cos[2\pi(f_r + f_{lo})t + (\phi_0 + \theta)] + \cos[2\pi(f_r - f_{lo})t + (\phi_0 - \theta)] \} \quad (3)$$

$$U_m = \frac{A_m A_{lo}}{2} \{ \cos[2\pi(f_r + f_{lo})t + (\phi_0 + \theta + \phi_x)] + \cos[2\pi(f_r - f_{lo})t + (\phi_0 - \theta - \phi_x)] \} \quad (4)$$

Two intermediate frequency signals can be obtained after low pass filtering, as shown below

$$E'_{ifr} = \frac{A_r A_{lo}}{2} \cos[2\pi f_i t + \phi_0 - \theta] \quad (5)$$

$$E'_{ifm} = \frac{A_m A_{lo}}{2} \cos[2\pi f_i t + (\phi_0 - \theta - \phi_x)] \quad (6)$$

Where  $f_i = f_r - f_{lo}$ .

It can be seen from equation (5) and (6) that the signals after frequency mixing remain phase-shift  $\phi_x$ , but signal frequency  $f_i$  is lower and it is therefore easier to obtain higher resolution phase measurement.

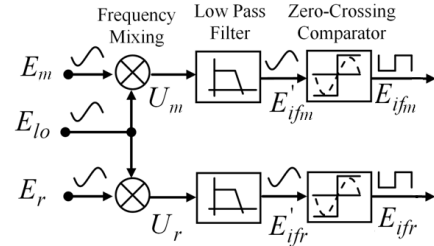


Figure 2. Heterodyne processing and digital conversion

After frequency mixing and low pass filtering, zero-cross comparators are used to convert sine wave signals  $E'_{ifr}$  and  $E'_{ifm}$  into square waves  $E_{ifr}$  and  $E_{ifm}$ . Then the task to measure phase-shift is also converted to measure the phase difference between two square waves.

#### 3.2 Dual channel digital phase measuring method

Dual channel digital phase measurement is shown in figure 3(a) and 3(b). With two measurement channels, the continuous gap-free phase measuring is available. In phase measuring channel 1, phase difference signal  $E_{ifd}$  is generated by signal  $E_{ifr}$  and signal  $E_{ifm}$  with the phase difference generation logic. Reference signal  $E_{ifr}$  is sent to the Gate control logic unit, which can divide the input frequency by a factor of two. Thus the gate control logic ensures the synchronization of gate signal with signal  $E_{ifr}$ , and its output is a 50% duty cycle square wave  $E_{gate}$ , whose period is equal to two cycles of  $E_{ifr}$ . In phase measuring channel 1, the whole cycle counter and the phase difference counter are enabled when the gate signal  $E_{gate}$  is at high level. As soon as the gate signal turns down, the whole cycle counter and the phase difference counter will be disabled. Supposed that their counts are  $N$  and  $M$  respectively, and then the phase shift between signal  $E_{ifm}$  and signal  $E_{ifr}$  is calculated by the micro processing unit (MPU)

$$\phi_x = 2\pi \cdot \frac{M}{N} \quad (3)$$

When the phase difference is calculated and exported by MPU, the whole cycle counting  $N$  and phase difference counting  $M$  are all set to zero in measuring channel 1. The next cycle counting will begin at once when the gate signal turn to high level again.

Be different from phase measuring channel 1, the whole cycle counter and the phase difference counter in phase measuring channel 2 are enabled when the gate signal  $E_{gate}$  is a low level and these two counters are disabled when the gate signal is at high level. By making the two phase measuring channels work in turn, a continue phase measurement is realized to avoid the error caused by missing pulses. Thus the update rate of whole dual-channel measuring system is equal to frequency of intermediate frequency signals  $f_i$ .

The dual channel digital phase measurement and control logic are all realized in FPGA. The standard pulse signal  $f_{cp}$  is frequency multiplied by  $K$  times with phase-locked loop (PLL) in FPGA, thus the frequency of actual counting pulse is  $Kf_{cp}$ .

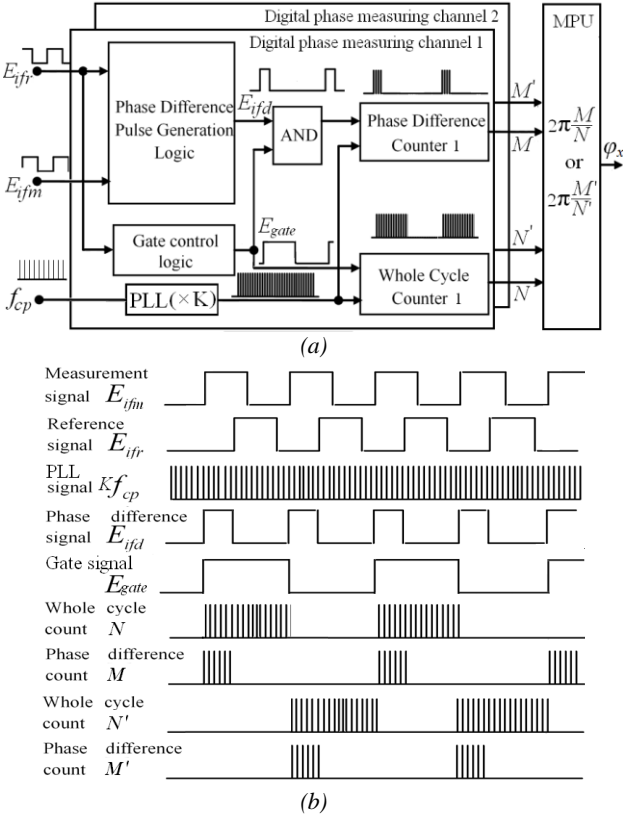


Figure 3. Two channel digital phase measurement  
(a) Block diagram, (b) Timing sequence

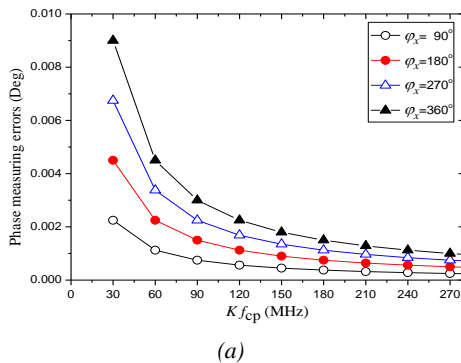
The measurement error of each digital phase measuring channel can be given by differentiating equation

$$\delta\varphi_x = 2\pi \cdot \left( -\frac{M}{N^2} \cdot \delta N + \frac{1}{N} \cdot \delta M \right) \quad (4)$$

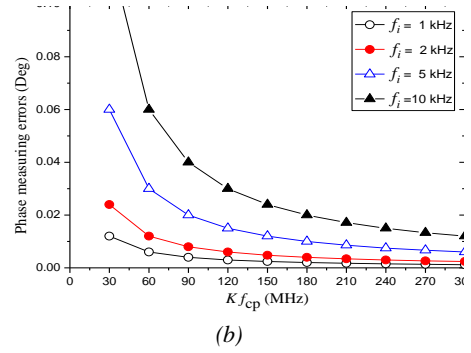
From  $N = Kf_{cp}/f_i$  and  $M = Kf_{cp}\varphi_x/(2\pi f_i)$ ,

$$\delta\varphi_x = 2\pi \cdot \left( -\frac{\varphi_x}{2\pi} \cdot \frac{f_i}{Kf_{cp}} \cdot \delta N + \frac{f_i}{Kf_{cp}} \cdot \delta M \right) \quad (5)$$

Equation (5) shows that the measurement error is caused by the counter error only, they are shown in figure 4(a) and 4(b) respectively. It can be seen that those two terms of error can be both less than  $10^{-2}$  degree due to  $\delta M_1 = \pm 1$ ,  $\delta M_2 = \pm 1$ , while  $Kf_{cp}$  is set at several hundreds of megahertz, and  $f_i$  set at several kilohertz, i.e.  $Kf_{cp} \gg f_i$ . Frequency drift of local oscillator and non-synchronization between gate signal and phase difference pulse signal have no influence on the measurement result. Moreover, the dual-channel digital phase measuring method improves the measuring rate up to 2 kHz while keeping the accuracy of phase measurement better than  $10^{-2}$  degree.



(a)



(b)

Figure 4. Inherent measurement errors of dual channel digital phase measurement. (a) Errors caused by  $\delta M$ , ( $f_i = 1$  kHz); (b) Errors caused by  $\Delta N$

### 3.3 Kalman filter based state estimation method

The phase measuring method mentioned above assumes the measurement end and active cooperative end are all static. However, there may be fast relative movement between these two ends in real conditions. On one hand, this causes change in frequency of measurement signal. On the other hand, the mean effect in phase measurement will induce dynamic errors. At the same time, the signal will be effected by noise from photodetection and circuit inevitably. And this causes random error in length measurement. To improve the measurement accuracy, these two errors should be reduced.

A state estimation method with errors pre-compensated based on Kalman filter is proposed to solve the problem of non-real-time measurement errors occurring in the phase-shift laser range finder system while measuring fast moving target. In this Kalman filter based method, the current non-real-time error is predicted according to the former state and the predicted-current state of the target, then the current non-real-time measurement error is compensated with the predicted value, and then, the current state of the target is estimated through the measurement value with pre-compensation by using the Kalman filter. With this kind of recursive estimation, state estimation of the target with high precision can be achieved when a new measurement value is obtained. The simulation results show that not only can this estimate effectively pre-compensate the non-real-time measurement errors caused by the movement of target, but also significantly reduce the influence of the random noise error of the measurement results.

## 4. Experimental results and analyses

Two types of experiments are presented to verify the validity of this method. The first one tests the static and dynamic accuracy by electronic simulation. Then a phase-shift laser ranging finder is established to test the static and dynamic accuracy of distance measurement.

### 4.1 Phase measuring unit test

Simulated signals from signal generators are used for most tests since they provide good accuracy and programmability and eliminate other sources of system error. The experimental setup shown in figure 5 is used to verify the effectiveness of the proposed high speed and high precision phase measurement. The measurement is realized in a field programmable gate array (FPGA) EP1C3T144, and computation is implemented in a digital signal processor (DSP) TMS320F2407A. Two phase-locked signal generators (Agilent 33220A) are employed to simulate the reference signal and the measurement signal, and another signal generator (Agilent 33120A) is employed to simulate the local oscillation signal.

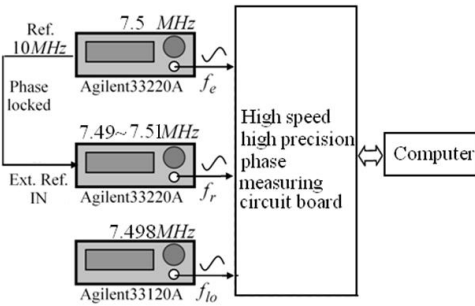


Figure 5. Experimental setup used for phase measurement

The static accuracy test applies a measurement signal while the phase is stepped from zero to 360° in 0.004° steps. At each phase step, 550 position readings are recorded. For each group of 550 readings, the mean and standard deviation are calculated. Figure 6 shows that the static resolution of phase measuring unit is better than 0.004°. As shown in figure 7, the phase measurement static accuracy is better than 0.012° in the range of zero to 360°.

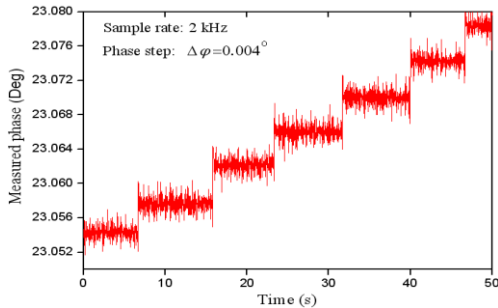


Figure 6. Phase measurement resolution test

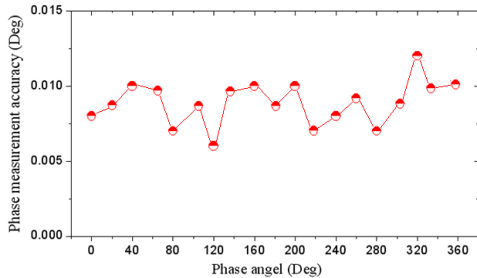


Figure 7. Phase measurement static accuracy vs. phase angle

The dynamic accuracy test uses two generators to simulate a stage moving at a constant velocity. One channel provides a fixed 7.5 MHz reference and the other channel is programmed to ramp up or down to the specified frequency. At each frequency, 50,000 positions and time data points are recorded and a least squares fit to a line is performed. The standard deviation of the position error between the line and the 50,000 points is recorded for each simulated stage velocity. The plot of the dynamic accuracy versus the velocity is shown in figure 8. Typical dynamic accuracy results are 0.012° near zero velocity and 0.02° at the velocity of 10m/s.

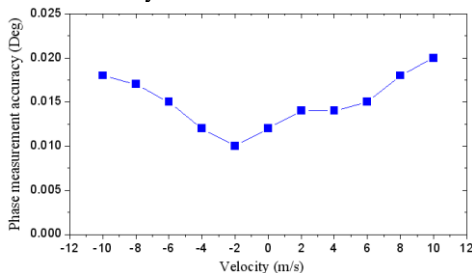


Figure 8. Phase measurement dynamic accuracy vs. velocity

#### 4.2 Phase-shift laser ranging finder test

The experimental setup used for laser range finder is as shown in figure 9. Transmitting and receiving optics employed is of coaxial structure. A laser diode with  $\lambda=650\text{nm}$  and  $P_{max}=10\text{ mW}$  is used as the laser source. An avalanche photo diode S2382 (Hamamatsu company) with  $S_{\lambda}=0.5\text{ A/W}$  is used as the optoelectronic detector. A cube corner reflector (CCR) is placed on the stage as the object, the stage can be moved along a rail with an accurate increment of 0.02mm and with maximum speed of 200mm/s.



Figure 9. Experimental setup of phase-shift laser range finder

In the experiment for static measurement accuracy, CCR moves away laser ranging finder with the step of 0.2 mm in a total range of 2 m. The computer samples the measurement result  $D_{LRF}$  and  $D_{LE}$  from the laser ranging finder and the linear encoder inside of the motion platform respectively. The static length measurement error can be obtained precisely by comparing the two results. As shown in figure 10, the distance measurement static accuracy is better than 1.2 mm at a data rate up to 2 kHz.

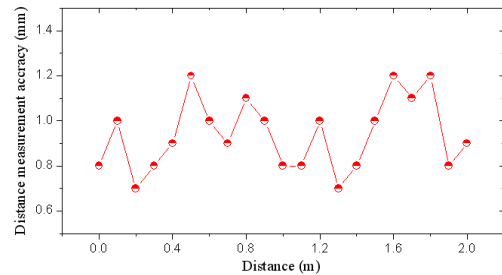


Figure 10. Distance measurement static accuracy vs. distance

To test dynamic measurement accuracy, CCR moves away laser ranging finder with the velocity of 200 mm/s in a total range of 2 m. Again, the computer samples the measurement result  $D_{LRF}$  and  $D_{LE}$  from the laser ranging finder and the linear encoder inside of the motion platform respectively. The dynamic length measurement error can be got in high precision by comparing the two results. According to data in figure 11, the length measurement uncertainty is less than  $\pm 1.2\text{ mm}$  ( $k=3$ ) when the target moves at the speed of 200 mm/s. Compared with static measurement accuracy, the dynamic measurement accuracy is not changed obviously. Limited by the velocity of motion platform, dynamic measurement experiment with higher velocity is not implemented.

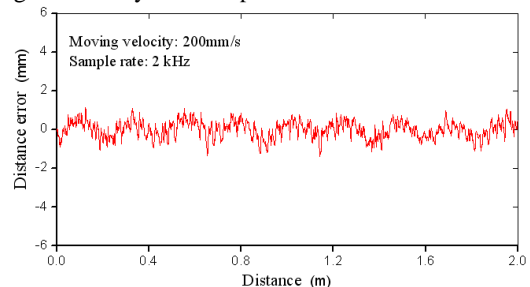


Figure 10. Distance measurement dynamic accuracy test

#### 4. Conclusions

It can be concluded from the results and discussion above that the proposed method can be used to enhance the measurement rate of phase shift laser range finder and to decrease the dynamic errors caused by motivation of measurement target in comparison with the conventional auto-digital phase measurement. For a target which moves at a velocity of 200 mm/s, a dynamic accuracy better than 1.2mm can be achieved at a data rate up to 2 kHz ( $t=0.5\text{ms}$ ) with the proposed laser range finder. To further test the dynamic accuracy of the proposed laser range finder, experimental setup with high speed motion platform will be built in later research.

#### ACKNOWLEDGEMENT

This research was supported by China Postdoctoral Science Foundation (CPSF: 20090450131) and the Research Fund for the Doctoral Program of Higher Education (RFDP: 20102302120006).

#### REFERENCES

1. Estler W. T., Edmundson K. L. and Peggs G. N., "Large-Scale Metrology – An Update," *CIRP Annals*, Vol. 51, No. 2, pp. 587-609, 2002.
2. Peggs G. N., Maropoulos P. G. and Hughes E. B., "Recent developments in large-scale dimensional metrology," *Proceedings of Institution of Mechanical Engineers, Part B*, Vol. 223, No. 6, pp. 571-595, 2009.
3. Kilpelä A., Pennala R. and Kostamovaara J., "Precise pulsed time-of-flight laser range finder for industrial distance measurements," *Rev. Sci. Instrum.*, Vol. 72, pp. 2197-202, 2001.
4. Heesun Y., Jinpyo H. and Seonggu K., "A multiple phase demodulation method for high resolution of the laser range finder," *3rd International Conference on Sensing Technology*, pp. 324-328, 2008.
5. Dupuy D., Lescure M. and Hélène T. B., "Analysis of an avalanche photodiode used as an optoelectronic mixer for a frequency modulated continuous wave laser range finder," *J. Opt. A: Pure Appl. Opt.*, Vol. 4, pp. s332-36, 2002.
6. Shahram M. N., Kiazand F. and Saeed O., "Modified Phase-Shift Measurement Technique to Improve Laser-Range Finder Performance," *Journal of Applied Sciences*, Vol. 8, No. 2, pp. 316-321, 2008.
7. Journet B. and Bazin G., "A low-cost laser range finder based on an FMCW-like method," *IEEE Trans. Instrum. Meas.*, Vol. 49, pp. 840-43, 2000.
8. Journet B. and Poujouly S., "High resolution laser range-finder based on phase-shift measurement method," *Proc. SPIE*, Vol 3520, pp. 123-32, 1998.
9. Liu S. Y., Tan J. B. and Binke H., "Multicycle synchronous digital phase measurement used to further improve phase-shift laser range finding," *Measurement Science and Technology*, Vol. 18, No. 6, pp. 1756-1762, 2007.